THE JOURNAL OF PHYSICAL CHEMISTRY C

ARTICLE

pubs.acs.org/JPCC

Highly-Controllable Molecular Imprinting at Superparamagnetic Iron Oxide Nanoparticles for Ultrafast Enrichment and Separation

Bianhua Liu,[†] Mingyong Han,[†,‡] Guijian Guan,[†] Suhua Wang,*[,†] Renyong Liu,[†] and Zhongping Zhang*[,†]

[†]Institute of Intelligent Machines, Chinese Academy of Sciences, Hefei, Anhui 230031, China

[‡]Institute of Materials Research and Engineering, 3 Research Link, A-STAR, 117602, Singapore

ABSTRACT: Here, we report a general protocol for coating molecularly imprinted polymers (MIPs) at the superparamagnetic iron oxide nanoparticles (Fe_3O_4 NPs) to make highly controllable core−shell Fe_3O_4@MIP NPs for rapid enrichment and separation of herbicides in water. Acrylic acid monomers were first anchored at the surface of Fe_3O_4 by the simple complexing reaction with unsaturated iron ions at the nanoparticle surface, which forms a polymerizable molecule monolayer. It was found that the monolayer highly directed the selective occurrence of molecular imprinting polymerization at the surface of Fe_3O_4 NPs, and the homogeneous copolymerization in solution phase was completely prohibited by the optimized reaction conditions. As a result, one can easily produce the uniformly spherical Fe_3O_4@MIP NPs with tunable MIP shell thickness from several to tens of nanometers that can simply be achieved by changing the amounts of precursors. The Fe_3O_4@MIP NPs with saturation magnetization of 38 emu/g exhibit the capability of ultrafast enriching and separating herbicide 2,4-dichlorophenoxyacetic acid (∼2% in weight) and are renewable and cyclically exploited due to their monodispersive and superparamagnetic features. The method of molecular imprinting at superparamagnetic particles can be extended to a wide range of applications for pollutant water treatment, biological molecule purification, and drug separation.

INTRODUCTION

Rapid enrichment and efficient separation of trace chemical species are very attractive techniques due to the huge commercial applications in water treatment,[1] biological molecule purification,[2,3] drug separation, and so forth.[4] Taking environmental pollutants, for instance, several million tons of herbicides and pesticides are used annually in agriculture across the world and thus cause various contaminations to natural water and groundwater, for which tens of herbicides/pesticides were found in the groundwater of the United States in the 1980s.[5] The organic pollutants in drinking water are currently removed by physical/chemical adsorption using active carbon, silica, or chemically modified adsorbents.[6−8] These materials are easily available but have to face the problems with low molecule selectivity, time-consuming procedures, and sophisticated equipments when used in water treatment.[1b] Moreover, the bad regeneration capacity largely increases the cost of practical operation. Likewise, liquid−solid extractions used widely in the protein and drug purifications also face these similar challenges.[9]

Magnetic nanoparticles have recently attracted considerable attention because of their potential applications in magnetic separation, biosensor, biological imaging, and drug delivery.[10−17] As one of the widest applications, superparamagnetic nanoparticles are the best candidate materials used as adsorbents in a simple, rapid separation of chemical species,[18] because the isolation and extraction of target molecules are extremely easy to handle by imposing an external magnetic field. In particular, the superparamagnetic nanoparticles can be redispersed by the removal of magnetic field and simple ultrasonication and can be cyclically regenerated and used by the removal of the attached analyte. However, the pure superparamagnetic nanoparticles such as Fe_3O_4 themselves may have several disadvantageous limitations: (1) the lack of molecular selectivity; (2) low binding capacity to target molecule; (3) spontaneous aggregation due to high surface energy; and (4) the lost of superparamagnetism when exposed to air.[19] Molecular imprinting at the surface of magnetic nanoparticles, which can coat the shell of molecularly imprinted polymers (MIPs) at the particle surface, not only keep the advantages of superparamagnetic particles but also effectively overcome these above shortcomings.[20]

MIPs have usually been regarded as artificial molecular recognition system like mimic enzymes[21] and were widely used in separation, chemosensor, and catalysis.[22−25] The molecular imprinting is conveniently done by embedding template molecules in a polymeric matrix through noncovalent/covalent interactions between templates and functional monomers.[26−28] The molecular recognition sites were generated by the subsequent removal of template molecules. As is well-documented in many places in the literatures,[29] coating the thin MIP shells at nanoparticles can provide the easy removal of template, high binding capacity, low mass transportation resistance, and fast binding kinetics. Up to date, the molecular imprinting at the

Received: June 7, 2011
Revised: July 17, 2011
Published: July 27, 2011

dx.doi.org/10.1021/jp205327q | J. Phys. Chem. C 2011, 115, 17320–17327

surface of magnetic particles has been carried out by two main methods: (1) the direct suspension of magnetic particles in the polymeric precursor solution;[30] (2) grafting initiator or chain-transfer reagent at the particle surface.[31,20b] Because of the uncontrollable feature for the surface polymerization, the highly uniform core−shell magnetic particles have rather rarely been reported.[32]

Here, we report a highly controllable and general protocol for coating molecularly imprinted polymers at the surface of superparamagnetic Fe_3O_4 NPs to make Fe_3O_4@MIP NPs for rapid enrichment and separation of herbicide 2,4-dichlorophenoxyacetic acid (2,4-D) in polluted water. 2,4-D is one of the most widely used halogenated agricultural chemicals around the world[33] and is notorious due to the persistence in the surface and ground waters and a well-known endocrine disrupter.[34] The World Health Organization (WHO) has recommended 30 μg/L as its maximum permissible concentration in drinking water.[35] Hence, the techniques for the removal of these trace organic pollutants/impurities by low-cost and rapid method are urgently needed for water safety and environmental protection. In our synthesis procedure, acrylic acid monomers were first anchored at the surface of Fe_3O_4 by the simple complexing reaction with unsaturated iron ions at the nanoparticle surface,[36] which forms a polymerizable molecule monolayer. The monolayer highly directed the selective occurrence of molecular imprinting polymerization at the surface of Fe_3O_4 NPs. The uniformly spherical Fe_3O_4@MIP NPs with tunable MIP shell thickness can simply be synthesized by changing the total amounts of precursors of MIPs.

EXPERIMENTAL SECTION

Materials. $FeCl_3 \cdot 6H_2O$, sodium acetate, ethylene glycol, polyethylene glycol (PEG, M_w = 2000), acrylic acid (Shanghai Chemicals Ltd.), and ethylene glycol dimethacrylate (EGDMA, Aldrich) were used as received. 2,4-Dichlorophenoxyacetic acid (2,4-D, Fluka), 4-chlorophenoxyacetic acid (4-CPA, Sigma), phenoxyacetic acid (PA, Sigma), and chlorpyrifos (CP, Sigma) were recrystallized with ethanol before use. Azo(bis)isobutyronitrile (AIBN) and acrylamide (AA, Shanghai Chemicals Ltd.) were purified through recrystallization in ethanol and acetone, respectively.

Synthesis of Fe_3O_4 NPs and Surface Modification. Uniform Fe_3O_4 NPs with diameters of ~200−300 nm were synthesized by the thermal decomposition of ferric chloride according to literature.[37] Typically, 1.35 g of $FeCl_3 \cdot 6H_2O$ was first dissolved in 40 mL of ethylene glycol to form a yellow clear solution. Samples of 3.60 g of sodium acetate and 0.10 g of PEG were then added to the above solution. After stirring for 30 min, the resultant solution was transferred into a Teflon lined stainless steel autoclave (50 mL). The autoclave was sealed and heated at 200 °C for 10 h, followed by cooling to room temperature. The black precipitate was collected and purified by washing sequentially with ethanol and deionized water for six times, respectively. The product (Fe_3O_4 NPs) was dispersed in ethanol with a concentration of 20 mg/mL for further use. The surface of Fe_3O_4 NPs was grafted with acrylic acid by the following procedure. Briefly, 5 mL of the suspension containing 100 mg of Fe_3O_4 NPs was added to 15 mL of ethanol under ultrasonication, followed by the addition of 20 μL of acrylic acid. The mixture was shaken at a rate of 300 rpm for 2 h. The acrylic acid monomers were anchored at the surface of Fe_3O_4 by the simple complexing reaction with unsaturated iron ions at the nanoparticle surface. The final product of Fe_3O_4-AA was separated and purified by magnetic collection and washing with ethanol and deionized water for three times, respectively. The purified Fe_3O_4-AA NPs can be dispersed well in organic solvent such as acetonitrile, chloroform, and dichloromethane. The existence of acrylic acid at the surface of Fe_3O_4 NPs was evidenced by the Fourier transform infrared (FT-IR) spectroscopy.

Molecular Imprinting of 2,4-D at the Surface of Fe_3O_4 NPs. Acrylamide and EGDMA were used as the functional monomer and cross-linking agent of the imprinting polymerization, respectively. Typically, 5 mL of the suspension containing 100 mg of Fe_3O_4-AA NPs was dispersed in 60 mL of acetonitrile by ultrasonication. Samples of 16.5 mg of acrylamide (0.23 mmol), 170 μL of EGDMA (0.90 mmol), 25 mg of 2,4-D (0.11 mmol) as the template, and 10 mg of AIBN (0.06 mmol) as the polymerization initiator were then mixed into the above suspension. The mixture was purged with nitrogen for 10 min while being cooled in an ice bath. A two-step polymerization was carried out in an incubating shaker with a rate of 300 rpm according to the following procedure. The prepolymerization was first done at 50 °C for 6 h, followed by normal polymerization at 60 °C for 24 h. The shell of 2,4-D imprinted polymer formed at the surface of Fe_3O_4 NPs. The product was then further aged at 85 °C for 6 h to obtain a high cross-linking density. The resultant Fe_3O_4@MIP NPs were magnetically separated and then sequentially washed with acetonitrile and ethanol. The thickness of the imprinted polymer shell was controlled by varying the total amount of the monomers including acrylamide and EGDMA. In all preparations, the mole ratio of acrylamide to EGDMA was kept constant at 0.25, while 100 mg of Fe_3O_4@MIP NPs was used. The corresponding nonimprinted core−shell particles were also synthesized by the identical procedure in the absence of 2,4-D template.

Measurements of Molecular Recognition Properties. The original templates, 2,4-D, in the polymer shell were extracted with a mixture of methanol and acetic acid (9:1, v/v) in a Soxhlet extractor. After template removal, the static binding capacity to the target analyte was measured by suspending 20 mg of Fe_3O_4@MIP NPs in the 10 mL mixture of methanol and water (7:3, v/v) with various 2,4-D concentrations. After incubation at room temperature for 12 h, the Fe_3O_4@MIP NPs in the solution were removed by magnetic separation. The binding amount of 2,4-D was determined by measuring the difference between the initial and the residual amounts in the solution on the basis of UV−vis absorption. Meanwhile, the binding kinetics was tested by monitoring the temporal evolution of 2,4-D concentration in the solutions.

Reusability for Magnetic Enrichment and Separation. A sample of 20 mg of Fe_3O_4@MIP NPs was suspended in 10 mL of the mixture of methanol and water (7:3, v/v) containing 2 mM 2,4-D. After incubation under a shaking table at room temperature for 30 min, the particles were separated from the liquid phase under a magnetic field. The concentration of 2,4-D residue in the liquid phase was determined by UV−vis absorption. The binding amount of 2,4-D was defined as the difference between the initial and residual amounts in the liquid phase before and after the treatment. The recovery of the 2,4-D uptaken by the Fe_3O_4@MIP NPs was determined according to the following procedure. The 2,4-D adsorbed at Fe_3O_4@MIP NPs was disassociated by suspending the magnetic particles in 5 mL of methanol/acetic acid (9:1, v/v), followed by incubation for 30 min. After the particles were separated under magnetic fields, the extraction

solution was dried with a nitrogen flow, and the residue was dissolved with 3 mL of methanol. The recovery amount of 2,4-D was finally determined by UV−vis absorption. The above procedures were repeated several times to validate the reproducibility and reusability of the imprinted nanoparticles for enrichment and separation.

Removal of 2,4-D in Lake Water and Tap Water. Lake water and tap water were chosen as the spiked matrices to evaluate the enrichment capability and the removal efficiency for 2,4-D by the Fe_3O_4@MIP NPs. The lake water and tap water were spiked with 2,4-D at the level of 5 μg/mL. A sample of 50 mg of Fe_3O_4@MIP NPs was added into 10 mL of the spiked lake water and tap water, respectively, followed by incubation for 30 min. The Fe_3O_4@MIP NPs were separated from the solution phase under the magnetic field, and the solution phases were collected for the concentration determination of 2,4-D residue using high-performance liquid chromatography (HPLC). The retention time and peak areas of 2,4-D in HPLC profiles were calibrated using 2,4-D standard solutions in methanol solvent (chromatographic grade) with concentrations at 0.01, 0.5, 1.0, 2.0, 5.0, 10.0, 50.0, and 100.0 μg/mL, which were prepared by diluting a stock solution of 1.0 mg/mL. The analytical column was a C_{18} column (250 mm × 4.6 mm inner diameter (i.d.)); the mobile phase was acetonitrile/water (60:40, v/v) at a flow rate of 1.0 mL/min, and the detection wavelength was 230 nm.

Characterizations. UV−vis absorption spectra were measured with a Shimadzu UV-2550 spectrometer. The morphologies and structures of the nanoparticles were examined by FEI Sirion-200 field emission scanning electron microscope. The X-ray diffraction pattern (XRD) was recorded on a MAC Science Co. Ltd. MXP 18 AHF X-ray diffractometer with monochromatized Cu Kα radiation (λ = 1.54056 Å). HPLC was performed on a Shimadzu CTO-10ASvp system consisted of a low-pressure gradient solvent pump, a manual operation-sampler, and a UV−vis detector. The magnetization measurements of the superparamagnetic Fe_3O_4 NPs at room temperature were performed with a SQUID magnetometer (MPMS-XL) from Quantum Design Corp.

RESULTS AND DISCUSSION

Protocol for Molecular Imprinting at the Surface of Fe_3O_4 NPs. Figure 1 illustrates the principle to synthesize Fe_3O_4@MIP NPs. First, Fe_3O_4 nanoparticle were functionalized with acrylic acid by a simple coordination reaction of carboxyl group of acrylic acid with the residual iron ions at the particle surface. As a result, the acrylic acid monomer was grafted to the surface of Fe_3O_4 particles, forming the molecule monolayer with polymerizable vinyl end groups. Subsequently, in the presence of functional monomer (acrylamide) and cross-linking agent (EGDMA), the acrylic acid monolayer will direct the selective occurrence of polymerization at the surface of Fe_3O_4 particles. Furthermore, the homogeneous polymerization in solution phase can completely be prevented by a stepwise polymerization via the slow prepolymerization at a low temperature and the normal polymerization at a relatively high temperature.[29] Therefore, the optimized reaction conditions finally lead to the formation of uniform polymer shells that are cross-linking matrix due to the coexistence of cross-linking reagent. Meanwhile, in the presence of 2,4-D template, the strong hydrogen-bonding interactions will occur between the amine group of acrylamide and the carboxyl group of 2,4-D. The template molecules were thus imprinted

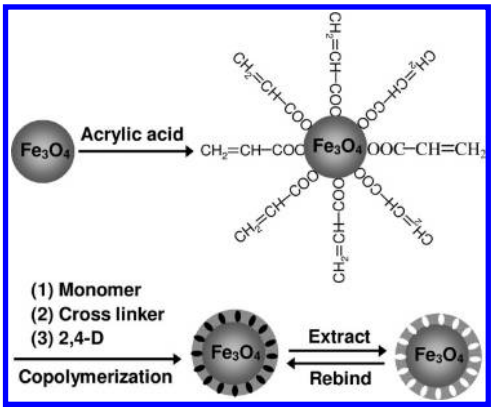

Figure 1. Schematic drawing for molecular imprinting at the surface of superparamagnetic Fe_3O_4 NPs.

within the matrix of polymer shells. After the template molecules (2,4-D) are removed by appropriate solvents to leave the cavities in the polymer shell, the resultant recognition sites can selectively rebind the target analyte because they are complementary in the shape, size and chemical interactions due to the memory effect of molecular imprinting.

Characterizations of Fe_3O_4 and Fe_3O_4@MIP NPs. Fe_3O_4 NPs were synthesized by the thermal decomposition of $FeCl_3 \cdot 6H_2O$ with the aid of ethylene glycol, which could obtain a high crystallinity and narrow size distribution. Figure 2A shows the scanning electron microscopy (SEM) image of synthesized Fe_3O_4 NPs. It can clearly be seen that the Fe_3O_4 particles with a size range of ∼200−300 nm in diameter are highly spherical and dispersive. Furthermore, as revealed by X-ray diffraction analysis (Figure 2B), the Fe_3O_4 particles are highly crystalline, face-centered cubic spinel. The diffraction peaks (2θ value) are indexed as (220), (311), (400), (422), (511), (440), and (533), respectively (JCPDS, 19-0629).[38] Meanwhile, FT-IR spectroscopy was used to characterize the chemical compositions of the bared, acrylic-acid-modified, and polymer-coated Fe_3O_4 NPs, respectively, as shown in Figure 3. The Fe−O stretching peak at ∼586 cm^{-1} was observed for three examples, indicating that the composition of Fe_3O_4 was not changed after chemical modification and polymer coating. The vibration band at 1728 cm^{-1} (C═O stretching) marked by black arrow in the spectra of acrylic-acid-modified Fe_3O_4 particles confirms the presence of C═O group and the successful modification of acrylic acid monomer. The intensity of C═O stretching (∼1728 cm^{-1}) was remarkably increased when Fe_3O_4 particles was covered with MIP that contains a large number of the C═O group in poly(acrylamide) units. Meanwhile, the strength of Fe−O stretching relatively decreased, due to the coating polymer shells at the Fe_3O_4 NPs. These observations clearly confirm the above synthesis mechanism and the occurrence of molecular imprinting polymerization at the surface of Fe_3O_4 NPs.

Control of Shell Thickness. We further examined the structure of Fe_3O_4@MIP NPs with SEM. Surprisingly, the product is highly spherical core−shell particles, in which Fe_3O_4 core and polymer shell on the every particles can be clearly distinguished as shown in the SEM images of Figure 4. Moreover, both pure polymer particles and bare Fe_3O_4 particles were not observed by careful SEM examinations. These further confirm the selective occurrence of imprinting polymerization at the surface of each Fe_3O_4 NPs with vinyl end groups. The thickness of the imprinted

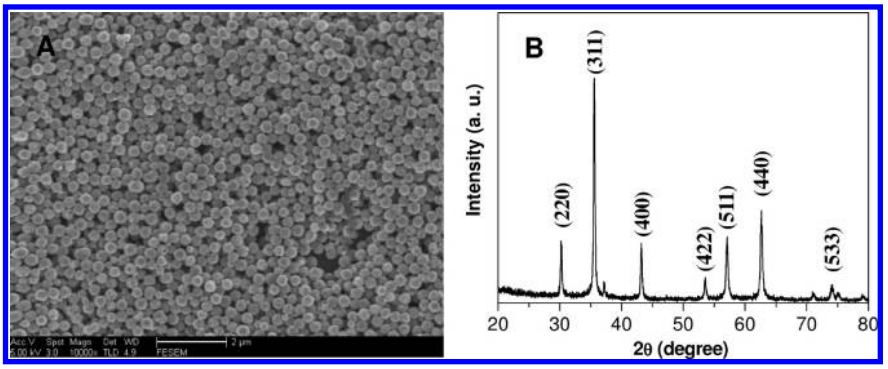

Figure 2. (A) SEM image of superparamagnetic Fe_3O_4 NPs obtained by a hydrothermal reaction at 200 °C for 10 h. (B) XRD pattern of synthesized Fe_3O_4 NPs (face-centered cubic lattice, JCPDS: 19-0629).

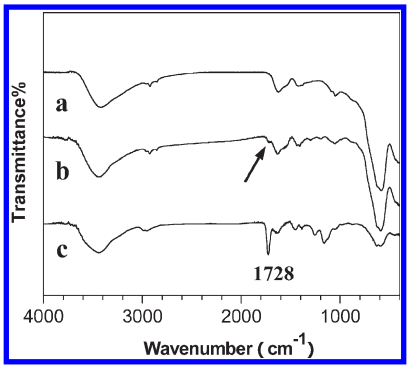

Figure 3. FT-IR spectra of (a) superparamagnetic Fe_3O_4 NPs, (b) the acrylic acid modified Fe_3O_4 NPs, and (c) Fe_3O_4@MIP NPs.

polymer shell can be tunable by controlling the total amount of the precursors. Typically, the shell thickness varies from 20, 30, or 60 to 120 nm when the total mass of the monomers changed from 0.15, 0.2, or 0.25 to 0.3 g, respectively (Figure 4A–D). However, the composite nanoparticles kept a perfect core–shell structure and were highly monodispersive with the increase of shell thickness. It should be noted that the uniform core–shell structures were not obtained when the total amount of precursor was large than 0.4 g because the homogeneous polymerization of the monomers unavoidably occurred in the solution phase. The resultant excessive polymer encased the Fe_3O_4 particles together to form large bulk aggregates.

Dependence of Rebinding Properties on Shell Thickness. The molecular recognition properties of the as-synthesized Fe_3O_4@MIP NPs with different shell thicknesses were investigated after the removal of the template molecules. We suspended the particles in the solution containing different 2,4-D concentrations. It can be detected that the equilibrium bound amount for Fe_3O_4@MIP NPs with different shell thickness gradually increased with 2,4-D concentrations (Figure 5A). The bound amount reached saturation as the concentration was 1 mM. On the other hand, the saturation capacity of Fe_3O_4@MIP NPs is dependent on the shell thickness. Clearly, the Fe_3O_4@MIP NPs with a 30 nm shell thickness show the highest saturation binding capacity. This result suggests that the 30 nm thickness may be a critical value to form the highest average density of effective imprinted sites in polymer shells which facilities the complete removal of templates and provides the easiest site accessibility to the target molecules.[29a] Furthermore, the mass of the imprinted polymer shells on the core–shell particles can be calculated according to the following equation:

$$M_{\text{shell}} = M \times \frac{(r_1^3 - r_2^3)\rho_p}{(r_1^3 - r_2^3)\rho_p + r_2^3\rho_m}$$

where M is the total weight of the Fe_3O_4@MIP NPs, r_1 and r_2 are the outer and inner radius of the core–shell particles, respectively, and ρ_p and ρ_m is the polymer and Fe_3O_4 densities, respectively. The densities of polymer shell and Fe_3O_4 nanoparticle core are adapted from their bulky values of 1.25 and 5.18 g/cm^3, respectively. For example, about 4.4 mg of the imprinted polymer is computed for 20 mg of the Fe_3O_4@MIP NPs with a 30 nm shell thickness. Therefore, the maximal rebinding capacity per milligram of MIP shells can be estimated from Figure 5A and is shown in Figure 5B. It is clear that the imprinted polymer shells have the similar highest rebinding efficiency when the thickness of the shell is less than 60 nm and exhibit the largest value (386 nmol/mg) at a 30 nm shell thickness. So, the Fe_3O_4@MIP NPs with a 30 nm shell thickness were chosen for further experiments on selective tests and practical separation of the target analyte from polluted water.

Figure 6A shows the adsorption abilities of the imprinted and nonimprinted nanoparticles toward target 2,4-D. The imprinted nanoparticles exhibited a much higher rebinding capacity than the nonimprinted ones. The saturated adsorption capacity to 2,4-D molecules by imprinted magnetic nanoparticles was calculated to be 85 nmol/mg (~2% in weight), which is about 2-fold of that by nonimprinted ones. Meanwhile, the rebinding kinetics of 2,4-D molecules were also investigated by changing the incubating time from 0 to 100 min, and the initial concentration of 2,4-D was kept constantly at 1 mM. The difference between the initial and residual amounts in the solution was monitored using UV–vis spectroscopy at a set time interval. Figure 6B shows that adsorption of Fe_3O_4@MIP NPs to 2,4-D analyte rapidly reached the saturated capacity in about 5 min. The rapid rebinding kinetics suggests an excellent application in ultrafast enrichment and separation of target species.

Selectivity of Fe_3O_4@MIP NPs to Analogous Compounds. We chose three typical pesticides including structurally analogous phenoxyacetic acid (PA) and 4-chlorophenoxyacetic acid (4-CPA) and structurally different chlorpyrifos (CP) for examining the molecular selectivity of 2,4-D-imprinted sites in the polymer shells (Figure 7A). Figure 7B shows the amounts of the analytes rebound by the imprinted nanoparticles and nonimprinted counterparts. It has been found that the imprinted nanoparticles exhibit a much larger binding capacity to 2,4-D

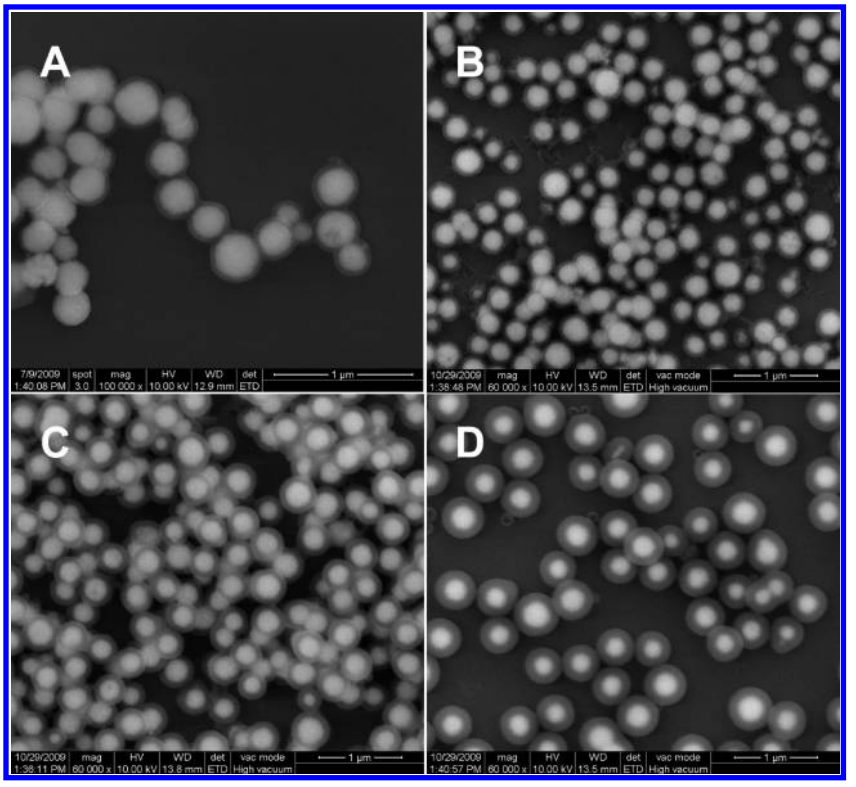

Figure 4. SEM images of Fe_3O_4@MIP NPs with different shell thickness: (A) 20, (B) 30, (C) 60, and (D) 120 nm.

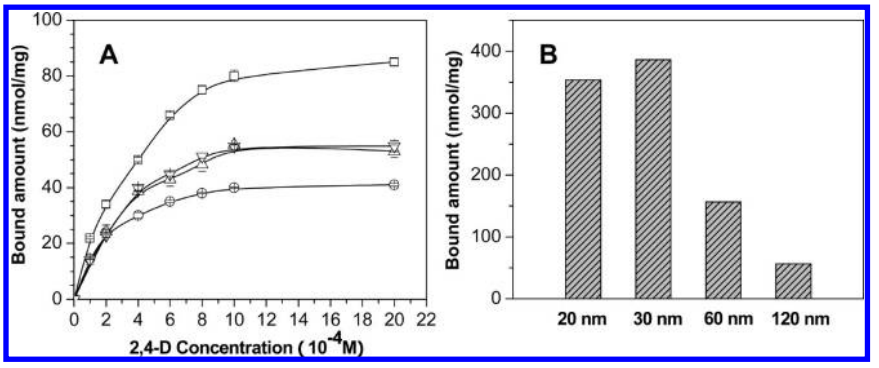

Figure 5. (A) Rebinding capacities to 2,4-D by Fe_3O_4@MIP NPs with different shell thickness, from top to bottom: 30, 20, 60, and 120 nm. (B) Maximal rebinding capacity of MIP shells vs thickness (data were calculated from the rebinding capacities at 2.0×10^{-3} M 2,4-D by Fe_3O_4@MIP NPs).

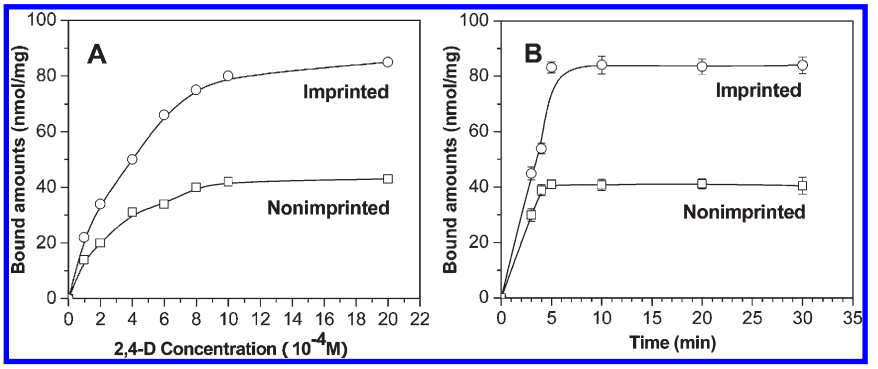

Figure 6. (A) Evolution of rebinding amount with 2,4-D concentrations and (B) the kinetics uptake to 2,4-D molecules by (○) the imprinted and (□) nonimprinted core−shell particles. The concentration of 2,4-D in kinetic test is 1 mM, and the shell thickness of core−shell particles is 30 nm.

dx.doi.org/10.1021/jp205327q |J. Phys. Chem. C 2011, 115, 17320–17327

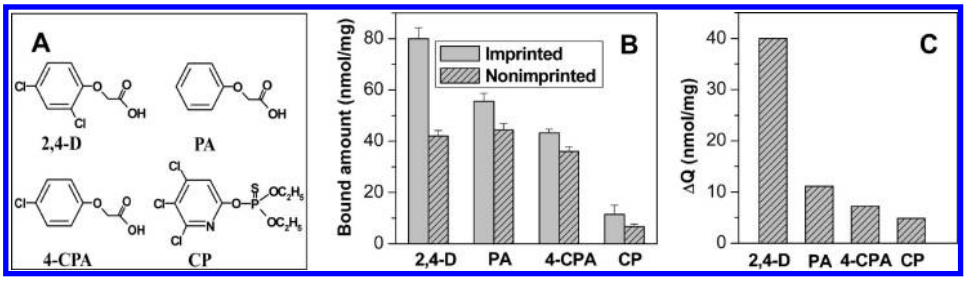

Figure 7. (A) Molecular structures of four typical pesticides. (B) Rebinding capacities of pesticides by the 2,4-D-imprinted and nonimprinted core−shell magnetic particles (30 nm shell thickness). All analyte concentrations are 1.0 mM. (C) Specific adsorption amounts of four pesticides at the 2,4-D-imprinted sites.

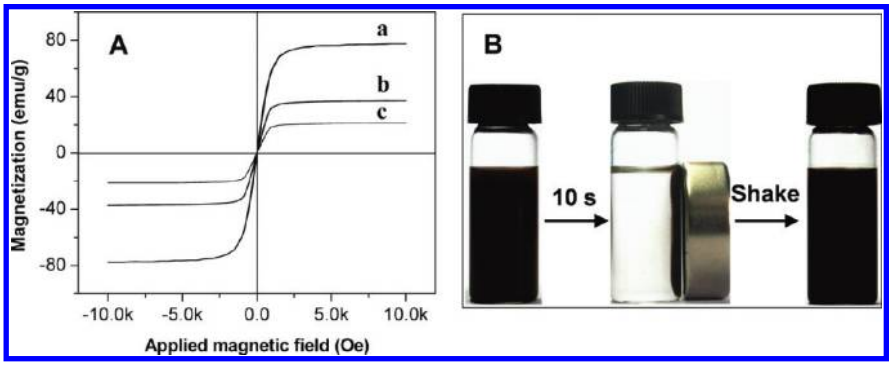

Figure 8. (A) Magnetization curves: (a) bared Fe_3O_4 NPs; (b) Fe_3O_4@MIP NPs (30 nm shell thickness); (c) Fe_3O_4@MIP NPs (120 nm shell thickness). (B) Magnetic response of Fe_3O_4@MIP NPs (30 nm shell thickness) to an external magnetic field.

than to the analogous PA and 4-CPA and an extremely low binding capacity to CP molecules. Meanwhile, the nonimprinted particles have a nearly similar capacity to rebind the three analogous molecules (2,4-D, PA, and 4-CPA) and a much smaller capacity to rebind the CP due to the lack of polar carboxyl group in CP molecule. Therefore, the differences in the rebinding capacities for imprinted or nonimprinted particles can reflect the specific adsorption amounts of four pesticides at the 2,4-D-imprinted sites, as shown in Figure 7C. It is clear that the imprinted sites exhibit a high selectively rebinding to 2,4-D target, which is about 4-, 5-, and 8-fold of those to PA, 4-CPA, and CP, respectively.

Magnetic Properties of Fe_3O_4@MIP NPs. Meanwhile, we investigate the magnetization of Fe_3O_4 before and after coating MIP shells by vibrating sample magnetometer. As shown in Figure 8A, there is no hysteresis in the magnetization curves of the bare Fe_3O_4 and Fe_3O_4@MIP NPs, regardless of the polymer shell thickness. Moreover, the magnetization curves are symmetrical and pass accurately through the origin, suggesting the remanence and coercivity are zero. These results suggest that Fe_3O_4 NPs are superparamagnetic, which facilitates magnetic separation and reusability. The saturation magnetization values were obtained as 78, 38, and 21 emu/g for bare Fe_3O_4 and Fe_3O_4@MIP NPs with 30 and 120 nm thickness shells, respectively. Although the increase of MIP shell thickness decreases their response to external magnetic field, the saturation magnetization value, for example, 38 emu/g for a 30 nm shell thickness, is still much higher to keep the superparamagnetic property as shown in other imprinted core−shell systems reported in literature.[20b,30,31] Furthermore, we observe the collection and redispersion process of Fe_3O_4@MIP NPs in solution in a vial by a small magnet. As shown in Figure 8B, the black NPs were drawn to the wall of vial within 10 s, resulting a clear and transparent solution. When the magnet was taken away and the vial was shaken gently, the black aggregates were well-redispersed. These further confirm that the Fe_3O_4@MIP NPs are highly superparamagnetic and have an excellent dispersibility.

Reusability for Magnetic Enrichment and Separation. The reusability of Fe_3O_4@MIP NPs is critical for magnetic enrichment and separation of target species from solution phase. We thus investigate the stability and reusability of the Fe_3O_4@MIP NPs by measuring the binding capacity and recovery efficiency to 2,4-D target in a cyclic manner. The binding amount of 2,4-D by Fe_3O_4@MIP NPs was tested by suspending the imprinted magnetic particles in 2,4-D solution for 30 min, and the particles were collected by a magnet. The recovery amount was determined by disassociating 2,4-D from these magnetic particles through acidic solvent (see Experimental Section). The adsorption and disassociation procedures were repeated several times for the identical batch of Fe_3O_4@MIP NPs to validate their reproducibility and reusability. Figure 9 presents cycles of rebinding−extraction processes, and the results show that the as-synthesized Fe_3O_4@MIP NPs have a high stability and remain almost the same abilities to bind target molecules even after six cycles, suggesting its potential practical applications in the treatment of polluted water.

Removal of 2,4-D in Real Water Samples. The imprinted superparamagnetic nanoparticles were evaluated on the ability of removing herbicide 2,4-D from lake water and tap water, respectively. Before the experiments, the lake water and tap water were spiked with 2,4-D at the level of 5 μg/mL. A sample of 50 mg of Fe_3O_4@MIP NPs was added into 10 mL of the spiked water, followed by incubation for 30 min. The imprinted particles were separated from the solution phase under a magnetic field,

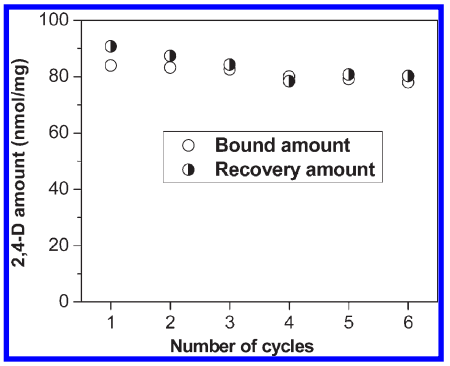

Figure 9. Cyclic rebinding and regeneration of Fe_3O_4@MIP NPs to 2,4-D. A sample of 20 mg of Fe_3O_4@MIP NPs and 2 mM of 2,4-D were used.

and the solution phases were collected for the concentration determination of 2,4-D residue using HPLC. The concentrations of 2,4-D residue in the solution phase were measured to be 0.34 μg/mL and 0.36 μg/mL in the lake water and tap water, respectively. The results show that the 2,4-D in the spiked water can be nearly completely removed. It should be noted that the very high concentrations of 2,4-D (5 μg/mL) is about 140-fold the maximum prescribed by EPA (30 μg/L).[35] By the first adsorption, about 93% of 2,4-D has been removed, suggesting a high removal capacity. If the water containing 0.34 μg/mL 2,4-D is treated once again with fresh Fe_3O_4@-MIP particles, the residue of 2,4-D is estimated to be 0.34 $\times$ (1−93%) = 0.024 μg/mL that is lower than the maximum threshold for acceptable drinking water. Therefore, the Fe_3O_4@MIP particles are potentially applicable in the treatment of drinking water. Moreover, the residues of 2,4-D in the lake water and the tap water are nearly the same, indicating that the impurities in the natural water do not interfere with the removal efficiency of 2,4-D.

CONCLUSIONS

In summary, we have developed a highly controllable and general protocol for coating molecularly imprinted polymers at the magnetic nanoparticles to make core−shell particles for rapid enrichment and separation of herbicides in water. The functional molecule monolayer can direct the molecularly imprinting polymerization selectively occurring at the surface of iron oxide nanoparticles. The thickness of imprinted shell is tunable in a wide range by changing the amount of polymerized precursors, and the magnetism is still kept at a relative high level. The imprinted magnetic particles could be easily and rapidly separated from the suspension under an applied external magnetic field. The imprinted particles could be used to specifically concentrate target molecules from large-volume environmental water samples with satisfactory recoveries and reproducibility. Although the current work is mainly focused on the imprinting of herbicide molecules, we have applied the imprinting technique to make various molecularly imprinted magnetic particles such as for environmental detrimental molecules atrazine and β-estradiol. The method of molecularly imprinting at magnetic particles can be extended to a wider range of applications in pollutant water treatment, biological molecule purification, and drug separation.

AUTHOR INFORMATION

Corresponding Author

*E-mail: zpzhang@iim.ac.cn (Z. P. Zhang); shwang@iim.ac.cn (S. H. Wang). Tel.: +86-551-5591654. Fax: +86-551-5591156.

ACKNOWLEDGMENT

This work was supported by Natural Science Foundation of China (Nos. 20807042, 21077108, 20925518, 30901008), China-Singapore Joint Research Project (2009DFA51810), National Basic Research Program of China (2011CB933700-03), and Innovation Project of Chinese Academy of Sciences (KSCX2-YW-G-058).

REFERENCES

(1) (a) Shannon, M. A.; Bohn, P. W.; Elimelech, M.; Georgiadis, J. G.; Mariñas, B. J.; Mayes, A. M. *Nature* **2008**, *452*, 301–310. (b) Renaud, E.; Romain, C.; Jean-Philippe, D.; Nicolas, B. *Water Res.* **2011**, *45*, 1–10.

(2) Davoli, E.; Fanelli, R.; Bagnati, R. *Anal. Chem.* **1993**, *65*, 2679–2085.

(3) Southard, G. E.; Houten, K. A. V.; Murray, G. M. *Macromolecules* **2007**, *40*, 1395–1400.

(4) (a) Sampson, J. S.; Hawkridge, A. M.; Muddiman, D. C. *Anal. Chem.* **2008**, *80*, 6773–6778. (b) Lei, Y.; Yang, S. K.; Wu, M. H.; Wilde, G. *Chem. Soc. Rev.* **2011**, *40*, 1247–1258. (c) Lei, Y.; Cai, W. P.; Wilde, G. *Prog. Mater. Sci.* **2007**, *52*, 465–539.

(5) Ritter, W. F. *J. Environ. Sci. Health, Part B* **1990**, *25*, 1–29.

(6) Liu, H. C.; Feng, S. P.; Du, X. L.; Zhang, N. N.; Liu, Y. L. *Energy Proc.* **2011**, *5*, 985–990.

(7) Bruggen, B. V.; Vandecasteele, C. *Environ. Pollut.* **2003**, *122*, 435–445.

(8) Matilainen, A.; Vepsäläinen, M.; Sillanpää, M. *Adv. Colloid Interface Sci.* **2010**, *159*, 189–197.

(9) Andersson, L. I. *J. Chromatogr., B* **2000**, *739*, 163–173.

(10) Zhang, L. M.; Zhang, K. Q.; Prändl, R.; Schöffl, F. *Biochem. Biophys. Res. Commun.* **2004**, *322*, 705–711.

(11) Dandamudi, S.; Campbell, R. B. *Biomaterials* **2007**, *28*, 4673–4683.

(12) Gao, X.; Yu, K. M. K.; Tam, K. Y.; Tsang, S. C. *Chem. Commun.* **2003**, 2998–2999.

(13) Teng, Z.; Li, J.; Yan, F.; Zhao, R.; Yang, W. *J. Mater. Chem.* **2009**, *19*, 1811–1815.

(14) (a) Kohler, N.; Sun, C.; Fichtenholtz, A.; Gunn, J.; Fang, C.; Zhang, M. *Small* **2006**, *2*, 785–792. (b) Chatzipavlidis, A.; Bilalis, P.; Efthimiadou, E. K.; Boukos, N.; Kordas, G. C. *Langmuir* **2011**, *27*, 8478–8485.

(15) Wan, J.; Cai, W.; Meng, X.; Liu, E. *Chem. Commun.* **2007**, 5004–5006.

(16) Shi, X.; Wang, S. H.; Swanson, S. D.; Ge, S.; Cao, Z.; Van Antwerp, M. E.; Landmark, K. J.; Baker, J. R. *Adv. Mater.* **2008**, *20*, 1671–1678.

(17) Fernández, B.; Gálvez, N.; Cuesta, R.; Hungría, A. B.; Calvino, J. J.; Domínguez-Vera, J. M. *Adv. Funct. Mater.* **2008**, *18*, 3931–3935.

(18) Laurent, S.; Forge, D.; Port, M.; Roch, A.; Robic, C.; Elst, L. V.; Muller, R. N. *Chem. Rev.* **2008**, *108*, 2064–2110.

(19) Alejandro, S. D.; Marta, E. D.-G. *Anal. Chim. Acta* **2010**, *666*, 1–22.

(20) (a) Ansell, R. J.; Mosbach, K. *Analyst* **1998**, *123*, 1611–1616. (b) Li, Y.; Li, X.; Chu, J.; Dong, C. K.; Qi, J. Y.; Yuan, Y. X. *Environ. Pollut.* **2010**, *158*, 2317–2323. (c) Tan, C. J.; Chua, H. G.; Ker, K. H.; Tong, Y. W. *Anal. Chem.* **2008**, *80*, 683–692.

(21) Haupt, K. *Analyst* **2001**, *126*, 747–756.

(22) (a) Wang, J. P.; Cormack, A. G.; Sherrington, D. C.; Khoshdel, E. *Angew. Chem., Int. Ed.* **2003**, *42*, 5336–5338. (b) Gai, Q. Q.; Qu, F.; Liu, Z.-H.; Dai, R.-J.; Zhang, Y.-K. *J. Chromatogr., A* **2010**, *1217*, 5035–5042.

(c) Riskin, M.; Ben-Amram, Y.; Tel-Vered, R.; Chegel, V.; Almog, J.; Willner, I. *Anal. Chem.* **2011**, *83*, 3082–3088.
(23) Wulff, G. *Angew. Chem., Int. Ed.* **1995**, *34*, 1812–1832.
(24) Liu, J. Q.; Wulff, G. *J. Am. Chem. Soc.* **2004**, *126*, 7452–7453.
(25) Liu, J. Q.; Wulff, G. *Angew. Chem., Int. Ed.* **2004**, *43*, 1287–1290.
(26) Yilmaz, E.; Haupt, K.; Mosbach, K. *Angew. Chem., Int. Ed.* **2000**, *39*, 2115–2118.
(27) (a) Xie, C. G.; Zhang, Z. P.; Wang, D. P.; Guan, G. J.; Gao, D. M.; Liu, J. H. *Anal. Chem.* **2006**, *78*, 8339–8346. (b) Xie, C. G.; Li, H. F.; Li, S. Q.; Wu, J.; Zhang, Z. P. *Anal. Chem.* **2010**, *82*, 241–249.
(28) Xie, C. G.; Liu, B. H.; Wang, Z. Y.; Gao, D. M.; Guan, G. J.; Zhang, Z. P. *Anal. Chem.* **2008**, *80*, 437–443.
(29) (a) Gao, D. M.; Zhang, Z. P.; Wu, M. H.; Xie, C. G.; Guan, G. J.; Wang, D. P. *J. Am. Chem. Soc.* **2007**, *129*, 7859–7866. (b) Guan, G. J.; Liu, R. Y.; Wu., M. H.; Li, Z.; Liu, B. H.; Wang, Z. Y.; Zhang, Z. P. *Analyst* **2009**, *134*, 1880–1886. (c) Liu, R. Y.; Guan, G. J.; Wang, S. H.; Zhang, Z. P. *Analyst* **2011**, *136*, 184–190.
(30) Hu, Y. L.; Li, Y. W.; Liu, R. J.; Tan, W.; Li, G. K. *Talanta* **2011**, *84*, 462–470.
(31) (a) Vestal, C. R.; Zhang, Z. J. *J. Am. Chem. Soc.* **2002**, *124*, 14312–14313. (b) Kan, X. W.; Zhao, Q.; Shao, D. L.; Geng, Z. R.; Wang, Z. L.; Zhu, J. J. *J. Phys. Chem. B* **2010**, *114*, 3999–4004.
(32) Chen, L. G.; Liu, J.; Zeng, Q. L.; Wang, H.; Yu, A. M.; Zhang, H. Q.; Ding, L. *J. Chromatogr., A* **2009**, *1216*, 3710–3719.
(33) Chu, W. *Chemosphere* **2001**, *44*, 935–941.
(34) Colborn, T.; Vomsaal, F. S.; Soto, A. M. *J. Environ. Health Perspet.* **1993**, *101*, 378–381.
(35) World Health Organization (WHO). World Health Organization: Geneva, 1998; Volume 2, pp 191−199.
(36) Sun, S.; Zeng, H.; Robinson, D. B.; Raoux, S.; Rice, P. M.; Wang, S. X.; Li, G. *J. Am. Chem. Soc.* **2004**, *126*, 273–279.
(37) Deng, H.; Li, X. L.; Peng, Q.; Wang, X.; Chen, J. P.; Li, Y. D. *Angew. Chem., Int. Ed.* **2005**, *44*, 2782–2785.
(38) Wang, C. Y.; Zhu, G. M.; Chen, Z. Y.; Lin, Z. G. *Mater. Res. Bull.* **2002**, *37*, 2525–2529.